International Journal of Mechanical, Industrial and Aerospace Sciences
ISSN: 2517-9950
Vol:10, No:3, 2016

Predicting Automotive Interior Noise Including Wind Noise by Statistical Energy Analysis

Yoshio Kurosawa

***Abstract*—**The applications of soundproof materials for reduction of high frequency automobile interior noise have been researched. This paper presents a sound pressure prediction technique including wind noise by Hybrid Statistical Energy Analysis (HSEA) in order to reduce weight of acoustic insulations. HSEA uses both analytical SEA and experimental SEA. As a result of chassis dynamo test and road test, the validity of SEA modeling was shown, and utility of the method was confirmed.

***Keywords*—**Vibration, noise, car, statistical energy analysis.

I. Introduction

RECENTLY, comfort in passenger car compartment has been much emphasized. We have to consider interior quietness even at design conception stage. The human ear is especially sensitive to the frequency range of 1000-4000 Hz and this range is classified as high-frequency interior noise. The main sources are engine and transmission noise during acceleration, tire pattern noise and wind noise for high-speed running vehicles. They are mainly air borne. Measures have been taken so far for these sources, but we also need to take measures on vehicle side (for acoustic insulation and absorption). In order to make noise small, soundproof materials more than 10 kg are used for one car. Besides this, recent fuel economy regulations have required auto manufacturers to reduce vehicle weight for better efficiency. In this condition, it is necessary to develop a high-precision technique and measures to predict high-frequency interior noise for good balance between quietness and weight reduction in automobile.

SEA [1], [2] has come to be used as prediction technology of high frequency interior noise. The SEA has the analytical SEA based on the theory type, and the experimental SEA based on the experiment. There is the hybrid SEA (HSEA) [3], [4] which combined these. HSEA is getting enough analysis precision for interior noise prediction by unite lump of the parameter which used the experimental results. But, input power was calculated from the chassis dynamo run, and wind noise was not able to be taken into consideration. Therefore, this research compared sound pressure level of test course run and chassis dynamometer (CDM) run. This research presented a modeling technique that uses the HSEA method. And this report shows the identification of materials properties of acoustic insulations, the desorption measurement and influence confirmation and modeling of the leak, CDM run and the comparison result of input analysis and the contribution degree analysis using the test course run trimming including the soundproof materials. This paper shows the contribution of reduction of weight for the soundproof materials.

Y. Kurosawa is with the Department of Mechanical and Precision Systems, Teikyo University, Utsunomiya, CO 327-8551 Japan (e-mail: ykurosawa@mps.teikyo-u.ac.jp).

II. Analysis Method

A. SEA

SEA is a method for predicting noise and vibration response in high-frequency range. This method describes interior noise and acoustic response by using energy and input power. The energy of vibration and acoustic response is calculated based on the balance of input power, damping loss power, and transmitted power for each subsystem. In this analysis, a statistical approach was adopted. It was assumed that acoustic and vibration mode is uniformly distributed in a given frequency band and is equally excited. From this way of thinking, the dissipated power in the subsystem of each frequency band is proportional to the subsystem energy level, and the transmission power is proportional to the energy level difference between the subsystems. When these relations in the case of two subsystems are summarized these in formula, it becomes (1):

$$\begin{pmatrix} P_1 \\ P_2 \end{pmatrix} = \omega \begin{pmatrix} \eta_1 + \eta_{12} & -\eta_{21} \\ -\eta_{12} & \eta_2 + \eta_{21} \end{pmatrix} \begin{pmatrix} E_1 \\ E_2 \end{pmatrix} \quad (1)$$

P_i: input power of subsystems i, E_i: energy of subsystems i, η_i: internal loss factor of subsystems i, η_{ij}: coupling loss factor from subsystems i to subsystems j, ω: angular frequency.

Internal loss factor and coupling loss factor are important parameters which are called SEA parameters and determine SEA model.

B. Analysis SEA Model

The SEA geometric model used by this calculation is shown in Fig. 1. Body panels, the floor, etc. which enclose car interior cavity (car room) were moderately divided so that the vibration or acoustic mode might fully exist with each subsystem in a high frequency range from 800 Hz to 5000 Hz; these are weak combination. These were made into the structure subsystems. Moreover, the vibration input parts (the body attachment parts of suspensions, engine mounts, and a propeller shaft) to the body were also modeled. We enclosed and divided air space layers within the body panels, which can be considered as acoustic subsystems. In this model, the structure subsystems are 106 subsystems, and ten subsystems of them are the input subsystems. Acoustic subsystems are 30 subsystems including the car interior cavity and engine room and trunk room. The trim, damping materials, soundproof materials, etc. were

laminated and modeled on the body panels (structure subsystem). In 5 mm pitch, the parts (floor carpet etc.) which have thickness distribution by the soundproof materials were changed gradually and modeled. Collectively, these constituted the analyzed SEA model.

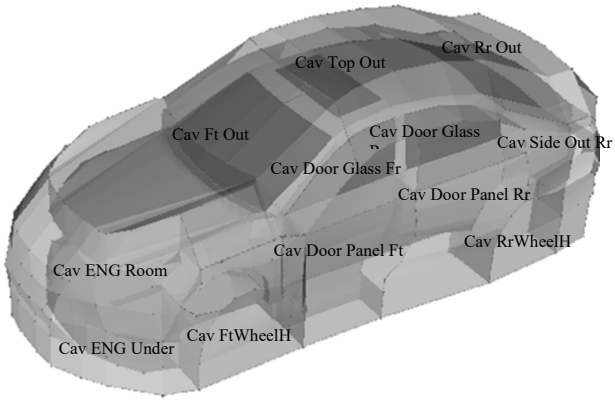

Fig. 1 Structure and acoustic subsystems of SEA model

C. Material Properties of Soundproof Materials

The car soundproof materials include glass wool (glass fiber), felt, and urethane foam. To build a model in analytical SEA, these material properties must be identified (parameters). Five parameters must be identified for glass wool or felt in an equivalent fluid model and nine parameters are required for polyurethane foam in the Biot model [5], [6]. But, the most important parameter for a sound performance is flow resistivity, the other values are determined by the soundproof materials used by car, and other influence of parameters is also small with it [4]. In this research, characteristic impedance and propagation constant are identified from the measurement which used the impedance tub [7], and the flow resistivity was calculated by the empirical formula of Delany-Bazley (2) [8]:

$$Z_c = \rho_0 c_0 \left[1 + 9.08X^{-0.75} - j11.9X^{-0.73}\right]$$
$$k = -j\gamma = \frac{\omega}{c_0}\left[1 + 10.8X^{-0.70} - j10.3X^{-0.59}\right] \quad (2)$$
$$X = \frac{\omega}{2\pi\sigma}$$

Z_c: characteristic impedance, ρ_0: air density, c_0: sound velocity, j: imaginary unit, σ: flow resistivity, γ: propagation constant.

The identification results for the flow resistivity relation and density are shown in Fig. 2 for the glass wool and felt at 2 kHz. From the results of having measured the glass wools and felts from which about ten kinds of densities differ, the relation (approximated curve in Fig. 2) of an exponential function was led to density and flow resistivity. Thereby, when predicting change of the sound pressure level in the car by the material substitution of soundproof materials, prediction became possible, without measuring an acoustic feature each time.

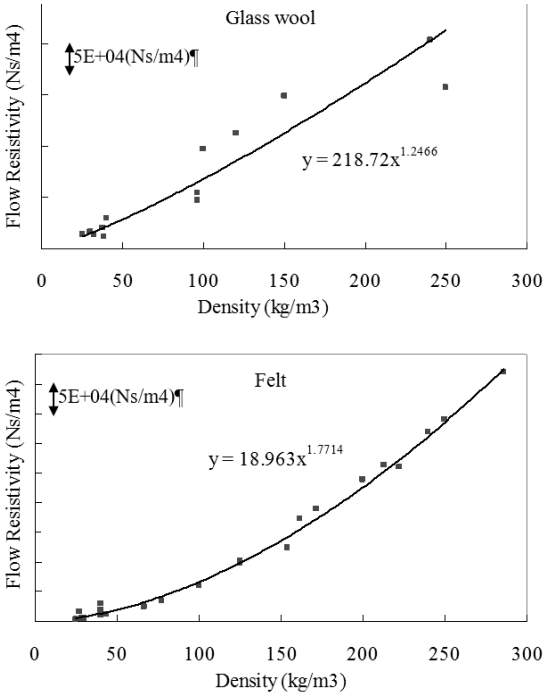

Fig. 2 Flow resistivity of glass wool and felt

Various shapes are on to secure strength and rigidity on a body panel. When laminating soundproof materials with pressure and cast original fabric of fixed thickness, the thickness distribution and densities also differ. Since flow resistivity will change if density changes, the sound absorption and the sound insulation also change. The experimental results and calculation results of transmission loss of toe board insulator (soundproof material laminated by the panel which separates a car room from an engine room) are shown in Fig. 3. Only the thickness distribution is taken into consideration in conventional modeling (Cal_old in Fig. 3). By considering the thickness distribution and density change (Cal_new in Fig. 3), we improved the calculation accuracy.

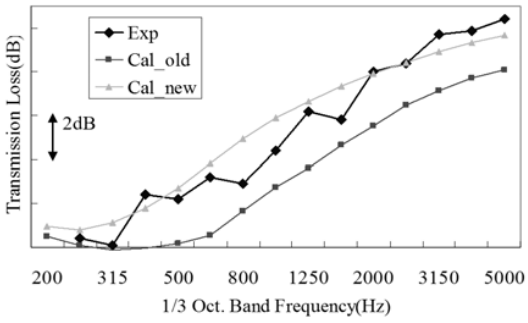

Fig. 3 Transmission loss of toe board insulator

D. Experimental SEA

The internal loss factor and the coupling loss factor for SEA parameters were asked for by experimental SEA. We used the internal loss factor ηi from (3) and input into the subsystem i

and the initial damping ratio β, as approximated from the reverberation curve [2].

$$\eta_i = \frac{\beta_i}{\omega} \tag{3}$$

Coupling loss factor η_{ij} was calculated from (4) by setting the energy response of the subsystem j at the time of inputting subsystem i to E_{ji} [2].

$$\eta_{ij} = \eta_j \frac{E_{ji}}{E_{ii}} \tag{4}$$

First of all, the value of η_{ij} in (4) were calculated for the maximum about two subsystems, and taking into consideration the influence of other contiguity subsystems, the unite lump was performed so that the sound pressure level finally emitted to interior cavity might suit the experimental results [2].

In the structure subsystems interval, the transfer functions were input using an impact hammer and measured with an accelerometer. The reply point assumed 3–5 points per a single subsystem and input around the reply points. The vibration speed was calculated and determined for each subsystem while the energy between the subsystems was calculated using (5):

$$E_i = M_i \left\langle |v_i|^2 \right\rangle \tag{5}$$

M_i: mass of subsystem i, $\left\langle |v_i|^2 \right\rangle$: mean-square value of vibration velocity (measurement results).

The acoustic subsystems carried the sound input using the speaker in the half-anechoic room. The sound pressure level was measured using a 1/4-inch microphone. The input position was based on 1-4 points per a single subsystem. Additionally, the answering point was based on 2–4 points per a single subsystem. The energy was then calculated from (6) using the measurement value [2]:

$$E_i = p_i^2 \frac{V_i}{\rho_0 c_0^2} \tag{6}$$

p_i: sound pressure level (measurement results), V_i: volume of subsystem i.

The interior cavity was measured using microphones located in the two passenger seat points (crew member lug position) and two backseat points (seat behind the passenger seat). A sound pressure level is defined as the averaged value between two points.

The SEA parameters for which these are asked inputted into the analytical SEA model, and the hybrid SEA model was created.

E. Trim Withdrawal Experiment, Modeling of Leak

Although the hybrid SEA model has been created by procedure, there are the crevices, variations, etc. of parts in actual vehicles. These variations cannot be disregarded when considering high frequency sound propagating through air. Therefore, the change in the sound pressure level in the car was measured with and without the floor carpet, seat or trim. The simulation was carried out on the SEA model, the crevice between parts and the air layer at the time of lamination were defined and the model accuracy was improved. A comparison of the experimental results regarding the change in the sound pressure level in the car and the calculation result (uniting after a lump) according to the underfloor speaker, with or without the rear seat cushion at the time of a sound pressure input, is shown in Fig. 4. Although early models provided experimental results and calculation results had a 5–10 dB difference, these calculations were determined with less than ±3 dB of errors due to realistic modelling of an actual vehicle based on the high frequency range (800–5000Hz). Therefore, the analysis accuracy at the time of weight saving examination was improved.

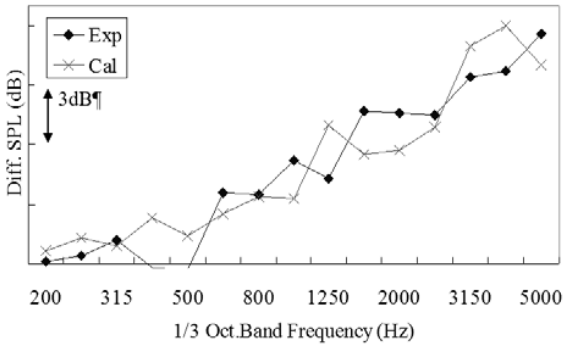

Fig. 4 Difference of sound pressure level from floor under to interior cavity with or without Rr seat cushion

The holes are vacant to let penetration parts pass on a toe board panel. Although the cap etc. has closed between the penetration parts and panel, these influences cannot be disregarded in a region of high frequency. The seals around all the holes were attached, the speaker input of the engine room was determined and then the difference in the interior cavity sound pressure level with and without the seal for each hole was measured. The transmission loss was defined and the circumference of each hole was modelled so that would be in agreement with measurement results (Fig. 5). Similarly, the air intake of the rubber seal around the circumference of each door and rear bumper is determined by experiment with or without a seal and modelled.

F. Measurement of Input Power

At the time of slow acceleration leading up to a 100 km/h regular run, the input power was measured for the sound pressure level of the acoustic subsystems of the left-hand side and centre (symmetry is assumed). Additionally, the input power was measured for the vibration level of 3–4 points per subsystems as a means of determining the vibration input to the body. Then the data computed every 1/3 octave band on a chassis dynamo (CDM) run and in a test course (TC) run and

subsequently averaged. The CDM was installed in the half-anechoic room and has the ventilation facility of the run style. Although the roller surface is flat, processing of the emery paper shape for slip prevention was provided. For the TC run, the acoustic subsystem outside the car was measured using the surface microphone as shown in Fig. 6. The TC road surface was asphalt and measurements at the time of a run were taken during the calm state.

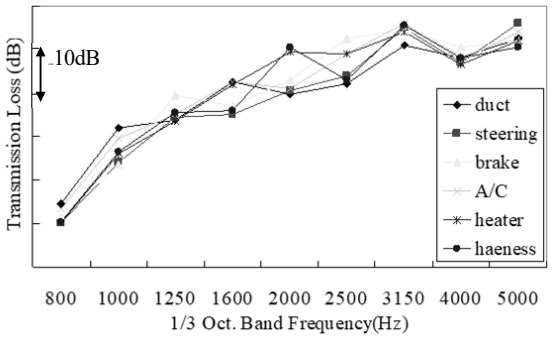

Fig. 5 Modeling for effect of holes

Fig. 6 Surface microphone

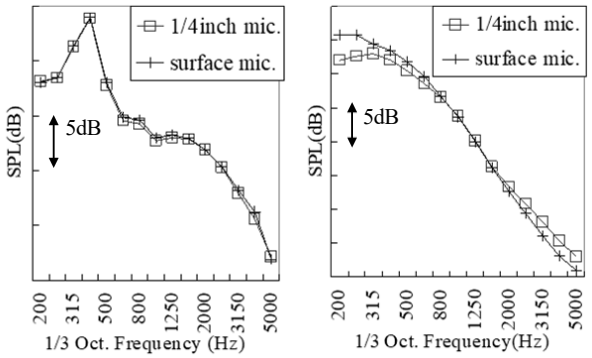

(a) In the time of stop (b) In the time of 100km/h run

Fig. 7 Comparison of sound pressure level of 1/4inch microphone and surface microphone

Comparison of the sound pressure level at the roof using the 1/4-inch microphone and a surface microphone is shown in Fig. 7. Although sound pressure levels are the same in the time of a stop (Fig. 7 (a)), the major difference occurs during the 100 km/h run (Fig. 7 (b)). This shows the influence of the window with the 1/4-inch microphone fixed to a body panel.

III. Calculation Results and Experimental Results

A. SEA Model Analysis Accuracy Check

Fig. 8 shows the comparison between the sound pressure level experimental results and calculation results in the seat next to the driver at the time of the 100km/h routine run in the TC. The difference in sound pressure level between the measurement and predicted value using this method was ±2 dB for the frequency range of 800−5 000Hz. The new modelling method was confirmed to have sufficient precision for examining weight reduction measures.

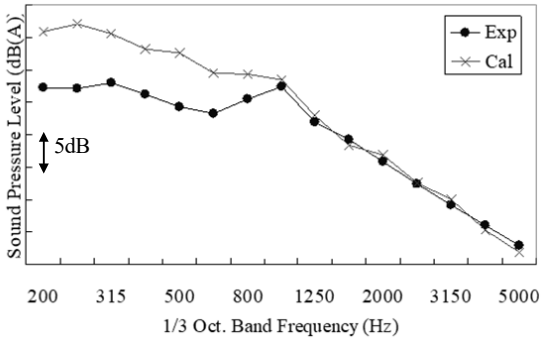

Fig. 8 Sound pressure level of interior cavity

B. Comparison of CDM Run and TC Run

Comparison of the measurement results of the sound pressure level for the 100 km/h regular run for the TC and CDM runs are shown in Fig. 9. The sound pressure levels are noted in a passenger seat (Fig. 9 (a)), a front door glass outside (Fig. 9 (b)), and a front tire house (Fig. 9 (c)). The level difference is significant for all frequency ranges for the front glass, door glass, outside door panel and roof, and is greatly influenced by wind noise as indicated in Fig. 9 (b). The sections inside of the wheel housings and engine room are seldom influenced by wind noise and the level difference was minor, as shown in Fig. 9 (c).

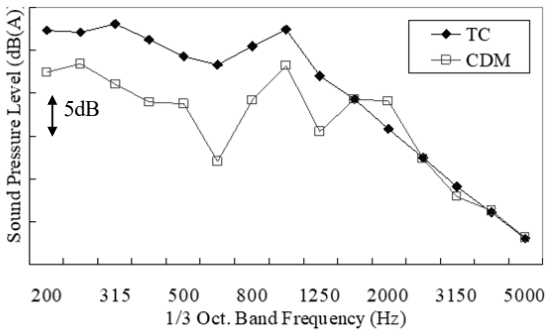

(a) 100km/h (Ft)

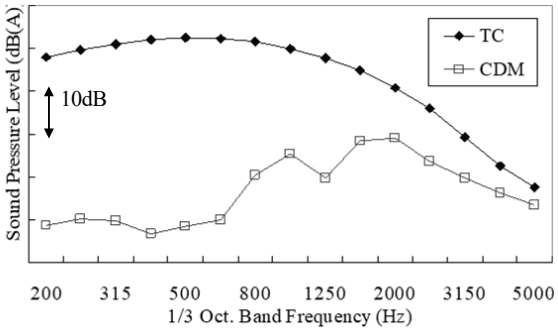

(b) 100km/h (Cav Door Glass Ft)

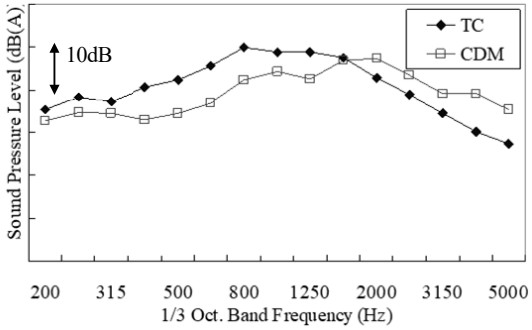

(c) 100km/h (Cav Ft WheelH)

Fig. 9 Comparison of sound pressure level of TC run and CDM run

The attribution analysis result of the input power to the passenger seat sound at the time of a 100 km/h regular run is shown in Fig. 10. Fig. 10 (a) shows the TC run, and Fig. 10 (b) shows the CDM run. The input power was calculated from the CDM measurement for the reason of not being conventionally influenced by the stability of a measurement value and the weather. Therefore, the influence of the wind noise from front door glass (Cav Door Glass Ft in Fig. 10) and windshield (Cav Ft Out in Fig. 10) were not able to be considered. The contribution of the vibration input (Structure in Fig. 10) was significant. Moreover, the factor is significant for underfloor (Cav Trunk Under and Cav Interior Under in Fig. 10) and wheel house (Cav Ft WheelH and Cav Rr WheelH in Fig. 10) at the time of a CDM run. As for the asphalt of the TC, an absorption coefficient is approximately 10–20% in a high frequency range. However, the floor of the half-anechoic room in which the CDM is installed is steel and concrete, which, therefore, does not absorb sound.

The comparison results of the contribution from each part of the interior cavity from the interior noise for the TC and CDM runs as averaged for the high frequency range are shown in Fig. 11. Fig. 11 (a) shows the passenger seat sound at the time of a 100 km/h regular run (Ft), Fig. 11 (b) shows the backseat sound (Rr), Fig. 11 (c) shows the passenger seat sound when the engine is rotating at 3000 rpm for slow acceleration (E/G). As Fig. 11 (a) indicates, the contribution from various parts such as Ft Glass, Door Glass Ft, Roof, etc. are influenced when the wind noise becomes significant and the attribution analysis result (Fig. 10) of input power, and the contribution of other parts is small. Also for Fig. 11 (b), the contribution from the glass becomes significant and contribution of the floor and Epron (i.e. panels of the circumference of back tires) are small. Moreover, the influence of Door Glass Ft is large but did not contribute in CDM run. In Fig. 11 (c), change in the TC and CDM runs is minor. These results are for speeds of approximately 50 km/h, and thus the influence of wind noise was seldom considered.

It was necessary to check and ask for input power from the TC run for conducting contribution analysis including the influence of wind noise.

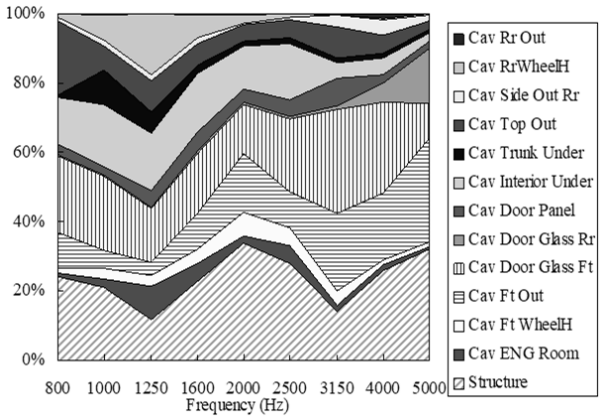

(a) 100km/h (Ft) : TC run

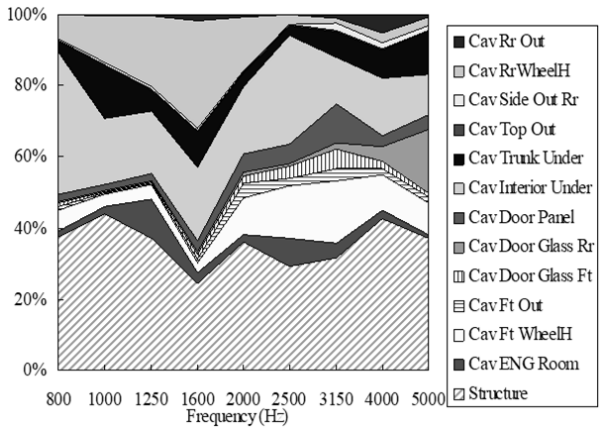

(b) 100km/h (Ft) : CDM run

Fig. 10 Contribution of input power

C. Contribution Analysis and Weight Saving Examination

The comparison results for the contribution for each part of interior cavity to interior noise by TC run and are averaged in the high frequency range as shown in Fig. 12. The figure shows that contribution changes greatly with run conditions or seat positions. By adjusting the balance of acoustic absorption and sound insulation, the specifications could almost maintain three performances. As a result, soundproof materials weight savings of about 500 g was determined.

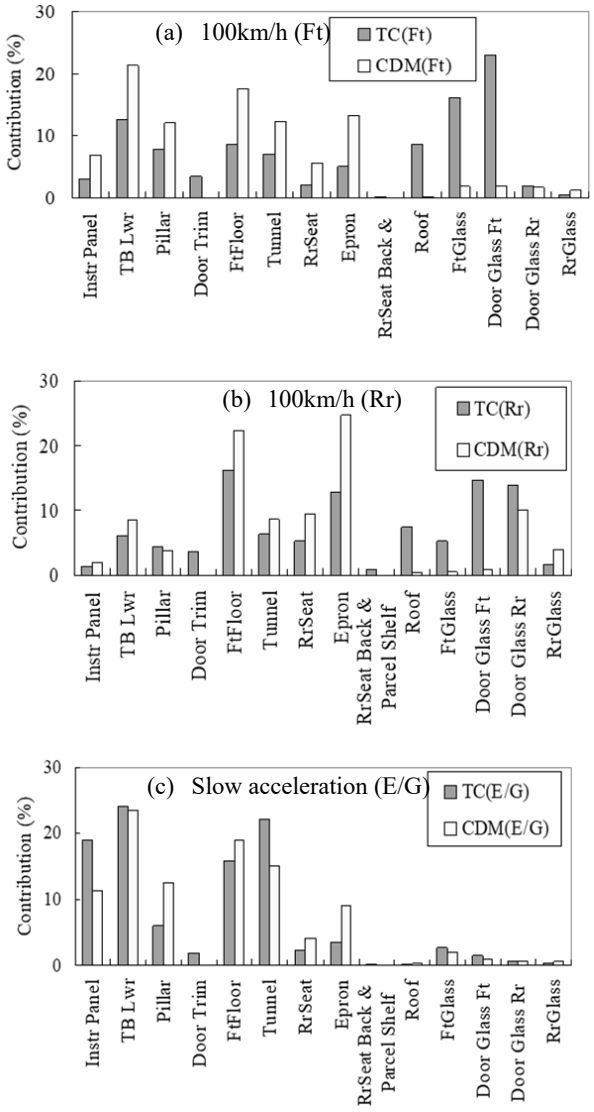

Fig. 11 Contribution to interior cavity sound pressure level

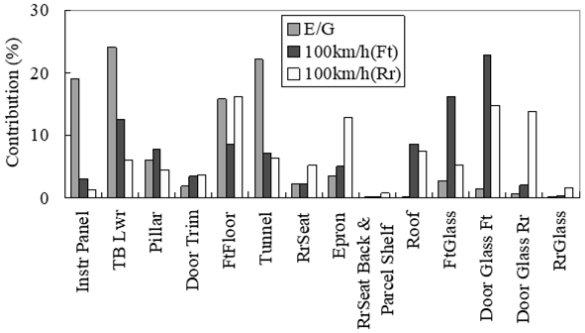

Fig. 12 Contribution to interior cavity sound pressure level

D. Analysis Accuracy Check by Real Run

The weight savings in soundproof materials was implemented in actual vehicles and the interior cavity sound pressure level was checked. A comparison of the measurement and calculation results is shown in Fig. 13. The difference of the initial specification and weight saving expectations of the interior cavity sound pressure level was determined. Fig. 13 (a) shows the passenger seat sound at the time of a 100 km/h regular run, Fig 13 (b) shows the backseat sound, Fig 13 (c) shows the passenger seat sound at the time of slow acceleration. A positive value indicates the aggravation of a sound pressure level. As for the difference of every band frequency, a tendency is slightly different from a measurement result in a calculation result. However, for the aggravation of the sound pressure level, even which driving condition is less than 0.5dB, it may be said that it is sufficiently small if it is considered as measurement error. Therefore, the usefulness of this technique has been checked.

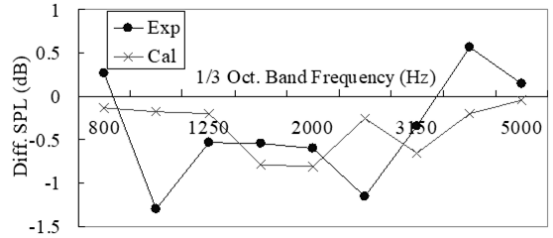

(a) TC (Ft)

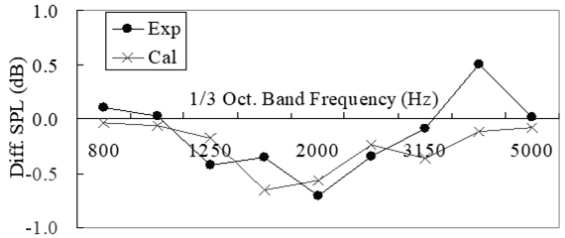

(b) TC (Rr)

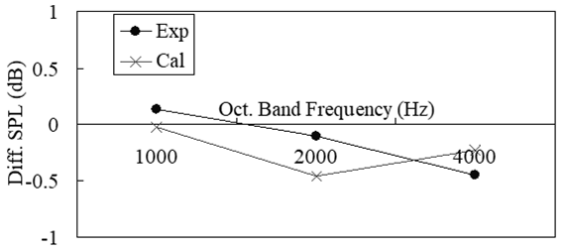

(c) TC (E/G)

Fig. 13 Difference of sound pressure level of interior cavity

IV. Conclusion

To perform a prediction of the sound pressure level in the high frequency range (800Hz−5000Hz) during a TC run for a car, the modelling technique using Hybrid SEA has been improved. Flow resistivity of the soundproof material was identified from the impedance tub measurement results, and the experimental expression of relations of flow resistivity and the density were determined. Analysis accuracy was improved by modelling with or without examination of the trim, soundproof

materials and leakage. The difference in sound pressure level was ±2 dB for the frequency range (800−5000 Hz) between the measurement and the prediction when using this method. The new modelling method has sufficient precision for examining weight reduction measures.

The contribution to interior cavity sound pressure level from input power or each car room part was measured during the CDM and TC runs. Although input power was conventionally identified from the CDM run, the attribution and contribution analyses containing wind noise were attained by identifying the TC run.

To study the reduction of weight of soundproof materials, the areas that make a significant contribution to front and rear seat respectively during acceleration and steady driving were identified. For these areas, the extent of effects with or without soundproof materials on the SEA model was calculated and optimised. Based on the results of the driving test, the application of weight reduction techniques without increasing the sound pressure level in the high-frequency range was confirmed.

REFERENCES

[1] Lyon R.H., Statistical Energy of Dynamical System, Theory and Applications, MIT Press, 1975.
[2] Lyon R.H., Dejong R.G.., Theory and Application of Statistical Energy Analysis, Butterworth-Heinemann, p. 277, 1995.
[3] Takahashi A., Nakane A., Hashigami S., Kokabu S., Misaji K., Vehicle Interior Acoustic Analysis by Hybrid SEA Method, Review of Automotive Engineering JSAE，No.54-10, 2010, pp.17-22.
[4] Kurosawa Y., Nakaizumi N., Weight Reduction Technique of Acoustic Insulation for Automobile Using SEA, Society of Damping Technology Symposium 2010, SDT10003, pp.11-16.
[5] Biot M.A., Theory of propagation of elastic waves in a fluid-saturated porous solid. Ⅱ. Higher frequency range, Journal of Acoustical Society of America, Vol.28, 1956, pp.179-191.
[6] Allard J.F., Propagation of Sound in Porous Media, Elsevier Applied Science, London and New York, 1993.
[7] Utsuno H., Tanaka T., Fujikawa T., Transfer Function Method for Measuring Characteristic Impedance and Propagation Constant of Porous Material, J. Acoust. Soc. Am. Vol.86, No.2, 1989, pp.637.
[8] Delany M.E., Bazley E.N., Acoustical properties of fibrous absorbent materials, Applied Acoustics 3, 1975, pp.105-116.